

MR thermometry using a paramagnetic lanthanide complex for evaluation of RF safety

S. Dharmadhikari^{1,2}, and N. Bansal^{1,2}

¹Purdue University, West Lafayette, Indiana, United States, ²Indiana University, Indianapolis, Indiana, United States

Introduction

Heating of tissues caused due to incident radio-frequency (RF) energy is a safety concern in MRI. RF-heating increases with field strength, is higher for certain sequences like $T_{1\rho}$ and may aggravate in the presence of conductive metallic implants which focus the eddy currents at the leads producing hot-spots. With increasing use and availability of implanted devices and MRI procedures, the safety evaluation of implants, pulse sequences and RF-devices for RF-heating has become critical. The quantity used to assess RF-heating is the rate of energy deposited in a mass of tissue termed as the Specific Absorption Rate (SAR). The recommended calorimetric method for evaluating SAR depends upon measurement of a small and linear temperature rise produced due to MRI over a short period of time and evaluating SAR using the model: $SAR = c \cdot dT/dt$ where dT/dt is the rate of change of temperature ($^{\circ}\text{C s}^{-1}$) and c is the specific heat capacity of the material ($\text{J kg}^{-1} \text{ } ^{\circ}\text{C}^{-1}$) [1]. Measurements of temperature using fiber-optic probes (FOPs) for calorimetry may vary significantly based upon the location, contact configuration and sensitive volume of the probe. Due to small RF-induced temperature changes (0.22°C in 15 min for SAR of 1 W/kg in tissue [1]) and spatial distribution of temperature, a method for imaging temperature with high temperature and spatial resolution is highly desirable. Thulium 1,4,7,10-tetraazacyclododecane-1,4,7,10-tetrakis(methylene phosphonate) (TmDOTP^{5-}), a paramagnetic lanthanide complex, has ~ 100 times strong chemical shift dependence on temperature ($C_T = 1.03 \text{ ppm}/^{\circ}\text{C}$) than water ($C_T = 0.01 \text{ ppm}/^{\circ}\text{C}$) (Figure 1). MR thermometry using TmDOTP^{5-} is also relatively insensitive to field inhomogeneities and system instabilities than water. The feasibility for absolute temperature imaging with a paramagnetic lanthanide complex both in phantoms and animals has been demonstrated [2]. The goals of this study were to apply MR thermometry using TmDOTP^{5-} for evaluating RF-heating during MRI and to develop a mathematical model for measurement of SAR. The temperature changes during MRI are a combined result of heating due to deposition of RF energy as well as heat dissipation to the surrounding. Currently recommended calorimetric methods for measurement of SAR do not consider heat losses due to conduction or convection [1] and may lead to an overestimation of SAR.

Methods

MR experiments were performed on a Varian 9.4-T, 31-cm diameter horizontal bore system using a 36-mm diameter quadrature birdcage coil consisting of 8 rungs. A cylindrical phantom filled with 50 mM TmDOTP^{5-} in 4% agarose gel was equilibrated to the surrounding overnight, to minimize thermal losses at the beginning of the experiment. Calibration experiments were performed by acquiring water and TmDOTP^{5-} spectra and by measuring temperature with FOP (accuracy = $\pm 0.05^{\circ}\text{C}$). Three-dimensional (3D) water and TmDOTP^{5-} images were collected using gradient echo (GE) imaging sequence with $TR = 100 \text{ ms}$ (water) or 10 ms (TmDOTP^{5-}) and $TE = 1.1 \text{ ms}$. 3D temperature images were calculated from phase shifts in TmDOTP^{5-} and water images using the relationship described in [2] and using the parameters obtained during the calibration. 3D SAR and cooling constant images were then computed on a voxel-by-voxel basis by curve-fitting the temperature data to the differential model: $dT/dt = [-k \cdot (T - T_a)] + (SAR/c)$, where dT/dt is the rate of change of temperature ($^{\circ}\text{C s}^{-1}$), k is Newton's cooling constant (s^{-1}), T and T_a are the measured phantom and ambient temperatures ($^{\circ}\text{C}$) and c is the specific heat capacity of the phantom material ($\text{J kg}^{-1} \text{ } ^{\circ}\text{C}^{-1}$). The ambient temperature was measured using a FOP placed in the proximity of the phantom throughout the experiment. A $T_{1\rho}$ imaging sequence with a spin lock (SL) pulse width = 0, 50 and 100 ms, $TR = 100 \text{ ms}$ and $TE = 1.1 \text{ ms}$ was evaluated. SAR measurements with a GE sequence were also repeated with a bare-ended insulated wire completely immersed in the phantom (Figure 3).

Results and Discussions

High SAR was observed near the walls of the phantom (Figure 2). The SAR was also higher specific to one side of the birdcage coil demonstrating possible heterogeneity in energy deposition (Figure 2). The $T_{1\rho}$ sequence known for its high SAR showed small but significantly higher mean SAR with increasing SL pulse duration (for SL = 0, 50 and 100 ms, SAR = 2.58, 3.13 and 3.52 W/kg respectively) (Figure 3). The SAR images for phantom with conductor showed hot spots near the bare end and higher mean SAR (Figure 4).

Conclusions

MR thermometry with TmDOTP^{5-} can provide accurate information about spatial temperature distribution, which will help to identify hot-spots and provide a good estimate of SAR over any given volume. Knowledge of ambient temperature provides more reliable model for SAR estimation by considering effect of heat loss. The use of TmDOTP^{5-} for SAR measurement in phantoms for evaluating implant safety is invaluable. Its application in human studies awaits further investigation.

References

[1] ASTM F2182-09 Standard Test Method for Measurement of Radio Frequency Induced Heating Near Passive Implants During Magnetic Resonance Imaging. *ASTM international*. [Online] [Cited: July 23, 2010.] <http://www.astm.org/Standards/F2182.htm> [2] James et al., *Magn Reson Med*, 2009, 62:550-556.

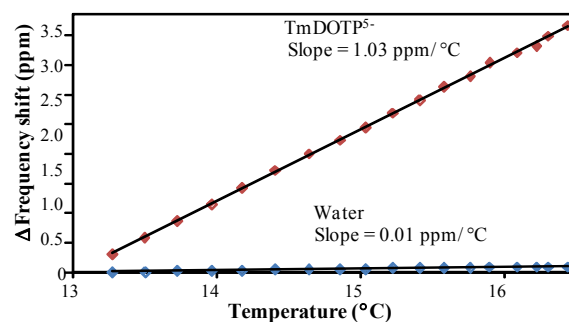


Fig 1. Comparison of temperature sensitivity of frequency shift for TmDOTP^{5-} and water.

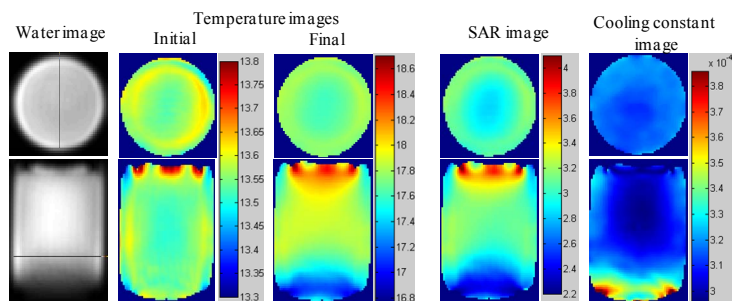


Fig 2. Representative slices of computed temperature, SAR and cooling constant maps for $T_{1\rho}$ sequence with SL = 50 ms.

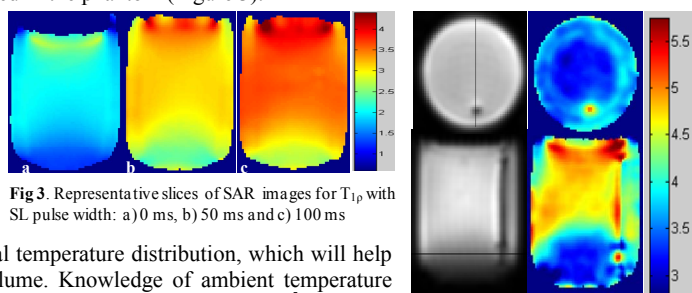


Fig 3. Representative slices of SAR images for $T_{1\rho}$ with SL pulse width: a) 0 ms, b) 50 ms and c) 100 ms

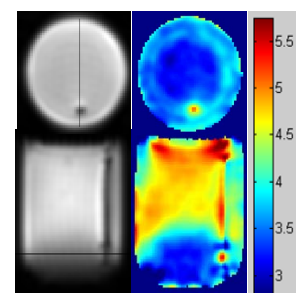


Fig 4. Representative slices of SAR image for a phantom with a conductor